Exp. Theo. NANOTECHNOLOGY 3 (2019) 213-220 https://doi.org/10.56053/3.2.213

Structural and optical properties of nanoparticulate Y_2O_3:Eu_2O_3

B. Klause[1,], G. Bremene[1], V. Hernn[2], A. Bosch[2]*

[1]Institute of Materials Physics, Graz University of Technology, 8010 Graz, Austria
[2]Karlsruhe Institute of Technology, Institute of Applied Materials—Materials Process Technology, 76344 Eggenstein - Leopoldshafen, Germany
*) Email: b.klause@tugraz.at

Received 10/1/2019, Accepted 25/2/2019, Published 15/5/2019

Nanoparticulate Y_2O_3:Eu_2O_3 with a small, uniform particle size and a well-defined composition was synthesized using a low temperature microwave plasma process. The structural evolution and the luminescence properties were studied in different states of annealing and Eu_2O_3 addition using X-ray diffraction, transmission electron microscopy, and UV-photoluminescence spectroscopy. As synthesized, the samples were amorphous and showed only weak luminescence. Subsequent annealing steps from 500°C to 800°C lead to the formation and growth of cubic Y_2O_3:Eu_2O_3 nanocrystals (5–20 nm) and a concomitant strong increase of the luminescence yield already at small grain sizes in the range of 10 nm. No self-quenching effects were observed up to 11 mol% Eu_2O_3.

Keywords: Structural; Optical; Nanoparticle.

1. INTRODUCTION

Luminescent rare earth oxides are in the focus of both technical application and ongoing research as key materials for use in display technology and lighting [1, 2]. Presently, Eu_2O_3, particularly in form of Y_2O_3:Eu_2O_3, constitutes the best red phosphor for fluorescence tubes and plasma display panels to convert UV light from the plasma discharge to red light [1, 3]. Y_2O_3 and Eu_2O_3 preferably form cubic mixed crystals with a high luminescence yield [1–5]. Both, the Y_2O_3 host lattice, and O^{2-} ions in the vicinity of Eu^{3+} ions, absorb UV-light with maxima in the range of 210 nm and 250 nm, respectively. Subsequent energy transfer to the Eu^{3+} luminescence centers finally populate the $5D_0$ level [1, 3–5]. Red light is emitted upon transition to one of the 7F levels, with the main emission line at 613 nm ($5D_0 \rightarrow F_2$)

and weaker lines between 580 and 595 nm [6]. The effect of a very small crystallite size on the luminescence properties, however, remains an open question. On the one hand, some studies report a noticeable blue shift of both the absorption range and the main emission line for particles as large as 40 nm [3, 7]. On the other hand, there are also observations of a red shift of the absorption spectra [4]. Sim- ilarly, studies in literature report observations of a reduced [1] as well as an increased luminescence of nanoparticles versus the bulk [8]. In addition, lattice and surface defects were found to significantly impair the luminescence yield of Y_2O_3:Eu_2O_3, particularly for very small particles [1, 3]. Therefore, Y_2O_3:Eu_2O_3 nanoparticles with a low degree of internal strains and agglomeration are expected to show im- proved luminescence. The present work aims at synthesizing and studying the structural and luminescence properties of such Y_2O_3:Eu_2O_3 nanoparticles with a small initial particle size. For this goal, microwave plasma (MWP) synthesis provides an ideal fabrication route [9]. The low reaction temperature of about 400°C and the electric charging in the nonequilibrium plasma leads to the formation of nanoparticles with both a small mean size of d ~4–5 nm and a narrow size distribution.

2 EXPERIMENTAL

The nanoparticulate Y_2O_3:Eu_2O_3 was produced by co- evaporation of the chemically homologous tetramethylheptanedionate Y(TMHD)$_3$ and Eu(TMHD)$_3$ precursors in an Arstream at about 180°C. The precursor vapor was mixed with a reaction gas of 20% oxygen in argon and then decom- posed in the microwave induced plasma (2.45 GHz, 500 W) under similar conditions as described for the synthesis of YSZ [9]. Electric charging induced by the plasma together with low reaction temperatures prevents the formation of hard agglomerates. The nanoparticles were collected on a cold finger. This powder was subsequently scraped off with a razor blade and placed in an Al_2O_3 boat for annealing treatments at temperatures between 350°C and 800°C in air. X-ray diffraction studies of the structural evolution of nanoscaled (n)-Y_2O_3:Eu_2O_3 powders were made using a Bruker D8 Advance instrument with a Cu tube. For trans- mission electron microscopy (TEM) studies using a Philips CM20 microscope, the n-Y_2O_3:Eu_2O_3 powder was dispersed in 2-Propanol and deposited on a Cu grid. Photoluminescence (PL) studies on n-Y_2O_3:Eu_2O_3 and the pure constituents were carried out on both powder samples on glass and dispersions in ethanol (0.5 g/l). The luminescence spectra were measured with a Perkin-Elmer LS55 spectrometer using a high-energy pulsed Xe

lamp as light source. A filter with a cut-off wavelength of 570 nm pre- vented spurious light from entering the analyzer. Two types of PL spectra were recorded for samples in all conditions of annealing and compositions: emission spectra of luminescence induced by excitation at fixed wavelengths of 211 and 234 nm and so-called excitation spectra, which show the intensity of the main PL emission line at 613 nm as a function of the excitation wavelength. A wavelength scan rate of 100 nm/min and bandwidths of 5 nm and 2.5 to 5 nm for excitation source and analyzer, respectively, were typically used for these measurements.

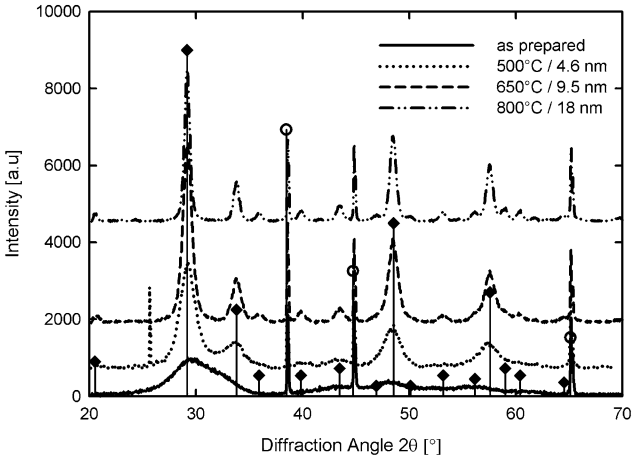

Figure 1 X-ray diffraction spectra of Y2 O3 :Eu2 O3 in different stages of annealing. The symbols F and denote literature data for Y2 O3 :Eu2 O3 (5 mol%) and Al (specimen holder) from the PDF-2 database, respectively [10]. No noticeable change is observed for sam- ples with Eu2 O3 addition of 5.6 and 11 mol%

3 RESULTS AND DISCUSSION

Under as-synthesized condition, both Eu_2O_3 doped (Figure. 1) and undoped Y_2O_3 nanoparticles show broad X-ray diffraction lines. In complementary TEM studies a small particle size and loose agglomerates of particles with nearly missing crystalline features were observed (Figure. 2a). Hence, an amorphous state with an average particle size of about 4.5 nm is deduced. Annealing at 350°C did not induce a significant change in the structural properties. Annealing at 500°C for 8 h lead to the formation of cubic nanocrystals of an Y_2O_3 :Eu_2O_3 solid solution (Figure. 1) or Y_2O_3, as shown by XRD. These data are consistent

with literature data for bulk $Eu_{0.1}Y_{1.9}O_3$ (JCPDS #25-1011) and Y_2O_3 (JPCDS #88-1040) in the PDF-2 database [10], respectively. No evi- dence for the formation of pure cubic Eu_2O_3 or monoclinic phases was found. From the XRD data, a small average crystallite size of 4.6 $\pm$ 0.5 nm is determined based on the Scherrer formula [11], whereas a detailed analysis using the approach of Williamson–Hall [11] yields a value of 6.5 $\pm$ 0.5 nm and indicates a noticeable amount of microstrains. Additional annealing at 650°C or 800°C (4 h) lead to crystallite growth reaching values of 9.5 $\pm$ 0.5 nm and 18 $\pm$ 1 nm, respectively. For samples annealed at 800°C, the crystallite size and the crystalline state was confirmed by TEM studies (Figure. 2b). Experimental data of the luminescence properties of Y_2O_3:Eu_2O_3 in dispersions are shown in Figures. 3, 4, and 5. In condition as synthesized and after annealing at 350°C, the n-Y_2O_3:Eu_2O_3 specimens showed only weak luminescence due the reduced energy transfer in the amorphous structure [12]. After annealing at 500°C, the typical luminescence spectrum of Eu^{3+} was observed (Figures. 3, 4).

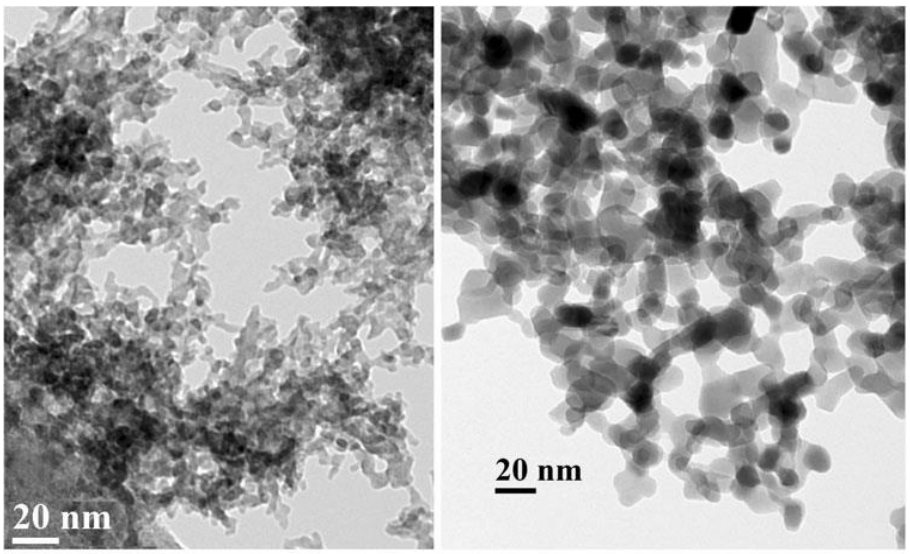

a b

Figure 2 TEM micrographs of (**a**) Y_2O_3:Eu_2O_3 as synthesized and (**b**) after the annealing step at 800°C (4 h, air)

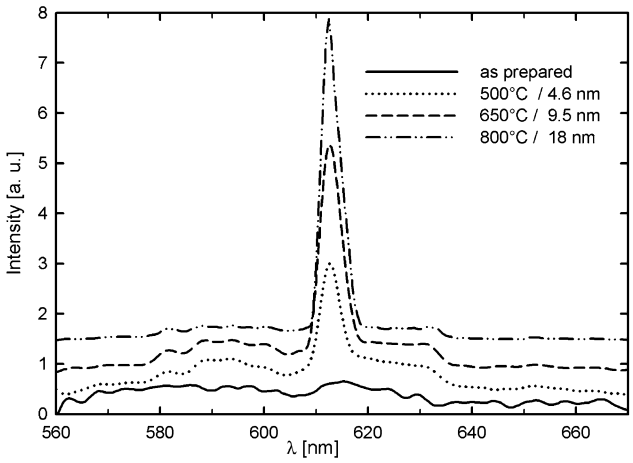

Figure 3 Luminescence spectra of n-Y2 O3 :Eu2 O3 (11 mol%) in disper- sion upon excitation with wavelength λex = 234 nm in different states of annealing. The plots are mutually shifted in vertical direction. The crystallite size is deduced from XRD line broadening (Scherrer Higher annealing temperatures of 650°C and 800°C led to a strong increase of the luminescence yield, but to no quali- tative change in the excitation and emission spectra such as shifts of the peaks with the grain size.

Taking into account the structural data (s. Figures. 1, 2) it may be concluded in agreement with literature data that a crystalline state is essential for the photoluminescence and UV conversion processes in Y_2O_3:Eu_2O_3 [3–7]. In fact, the PL yield is reduced for ultra-small grain sizes (Figures. 3–5). However, we observed a significant PL yield already at crys- tallite sizes in the range of 5–10 nm (Figure. 3), smaller than previously reported [3].

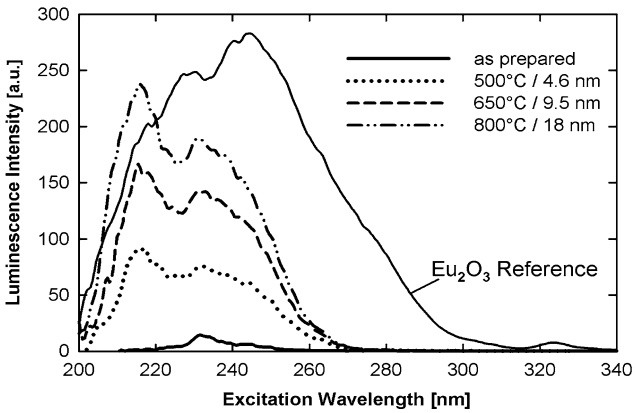

Figure 4 Excitation spectra for the luminescence at λ_{em} = 613 nm($^5D_0 \rightarrow {}^7F_2$) measured on dispersed Y_2O_3:Eu_2O_3 particles. Bulk Eu_2O_3 is shown as a reference

A detailed look at the excitation spectra of n-Y_2O_3:Eu_2O_3 specimen (Figure. 4) shows two maxima for wavelengths of about 211 nm and 234 nm in the far UV range, which can be attributed to the host-lattice and charge transfer mechanisms, respectively [3–5]. The PL yield for both excitation wavelengths increase with the grain size (Figure. 4, Figure. 5) as well as with the Eu_2O_3 content (Figure. 5). Hardly any PL is observed for the as prepared n-Y_2O_3:Eu_2O_3 specimen at λ_{ex} < 220 nm (Figure. 4). With higher annealing temperatures and crystallite size the excitation at λ_{ex} = 211 nm, corresponding to the host lattice transfer, becomes more dominant in comparison to λ_{ex} = 234 nm, which may reflect a more efficient host-lattice energy transfer in larger grains [1, 3–5]. It is also interesting to note, that the relative intensity of the main emission line, which is attributed to Eu^{3+}.

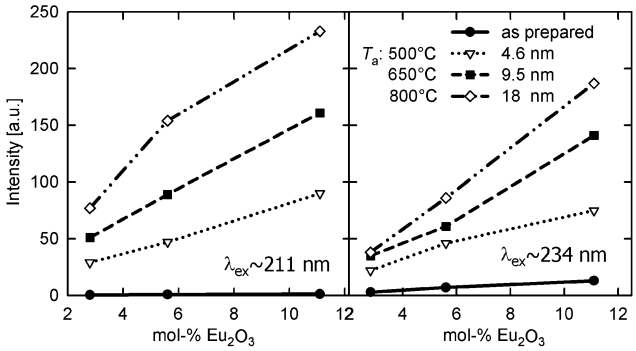

Figure 5 Variation of photoluminescence yield in Y_2O_3:Eu_2O_3 with annealing treatment and Eu_2O_3 content for regions of host lattice(λ_{ex} = 211 nm) and charge transfer excitation (λ_{ex} = 234 nm)

Emission centers in an undistorted cubic lattice environment [13], increases for higher annealing temperatures (Figure. 3). These improved luminescence properties may be at- tributed to a reduced density of lattice and surface defects as a result of the synthesis method used [12]. No evidence for self-quenching was observed for any state of annealing or Eu_2O_3 content up to the highest doping level of 11 mol% studied. For bulk material, such a quench- ing effect was reported for Eu_2O_3 additions to Y_2O_3 as low as 6% [14]. Assuming an isotropic distribution of Eu^{3+} in the nanocrystals, the reduced self-absorption may be at- tributed to the large fraction of luminescence centers located directly at the nanoparticles' surface, which is expected to reduce this doping-dependent critical effect. Based on these results, it can be concluded that mi- crowave plasma synthesis combined with appropriate annealing is a powerful technique for the fabrication of ox- ide rare earth nanoparticles, which combine a well-defined small size and composition with good luminescence prop- erties. Nevertheless, the present study confirms that the luminescence yield of Y_2O_3:Eu_2O_3 is reduced for very small grain sizes. Slightly larger grains (d ≥ 9.5 nm) with a high degree of crystallinity show a promising luminescence yield tendency.

Acknowledgements: The authors thank A. Meingast, Graz University of Technology, for TEM micrographs and S. Draxler, University of Graz for technical support.

References

[1] R. Schmechel, M. Kennedy, H. von Seggern, H. Winkler, M. Kolbe, R.A. Fischer, Li Xaomao, A. Benker, M. Winterer, H. Hahn, J. Appl. Phys. 89 (2001) 1679
[2] P.K. Sharma, M.H. Jilavi, R. Nass, H. Schmidt, J. Lumin. 82 (1999) 187
[3] A. Konrad, T. Fries, A. Gahn, F. Kummer, U. Herr, R. Tidecks, K. Samwer, J. Appl. Phys. 86 (1999) 3129
[4] Q. Meng, C. Qingyu, B. Chen, X. Zhao, X. Wang, W. Xu, J. Nanosci. Nanotechnol. 8 (2008) 1443
[5] A. Konrad, U. Herr, R. Tidecks, F. Kummer, K. Samwer, J. Appl. Phys. 90 (2001) 3516
[6] G. Wakefield, E. Holland, P.J. Dobson, J.L. Hutchison, Adv. Mater. 13 (2001) 1557
[7] Q. Li, L. Gao, D. Yan: Nanostruct. Mater. 8 (1997) 825
[8] E.T. Goldburt, B. Kulkarni, R.N. Bhargava, J. Taylor, M. Libera, J. Lumin. 72–74 (1997) 190
[9] U. Brossmann, M. Sagmeister, P. Pölt, G. Kothleitner, I. Letofsky- Papst, D.V. Szabó, R. Würschum, Phys. Status Solidi RRL 1 (2007) 107
[10] PDF-2, The Powder Diffraction File Rel. 2001 (The International Center for Diffraction Data, Newtown Square, (2001)
[11] H.P. Klug, L.E. Alexander, X-ray Diffraction Procedures for Poly- crystalline and Amorphous Materials, 2nd edn. (Wiley, New York, (1974)
[12] R. Schmechel, H. Winkler, Li Xaomao, M. Kennedy, M. Kolbe, A. Benker, M. Winterer, R.A. Fischer, H. Hahn, H. von Seggern, Scr. Mater. 44 (2001) 1213
[13] M. Mourad Mabrook, Exp. Theo. NANOTECHNOLOGY 2 (2018) 103
[14] X. Ye, W. Zhuang, Y. Hu, T. He, X. Huang, C. Liao, S. Zhong, Z. Xu, H. Nie, G. Deng, J. Appl. Phys. 105 (2009) 064302